TISSUE ENGINEERING: Part A
Volume 18, Numbers 1 and 2, 2012

DOI: 10.1089/ten.tea.2010.0731

Hypoxia Impedes Vasculogenesis of *In Vitro* Engineered Bone

Debby Gawlitta, Ph.D.,[1] Joost O. Fledderus, Ph.D.,[2] Mattie H.P. van Rijen, B.Sc.,[1] Inge Dokter, B.Sc.,[1] Jacqueline Alblas, Ph.D.,[1] Marianne C. Verhaar, M.D., Ph.D.[2] and Wouter J.A. Dhert, M.D., Ph.D.[1,3]

To ensure the survival of engineered bone after implantation, we combined human endothelial colony forming cells (ECFCs) and multipotent stromal cells (MSCs) as a proof of concept in a co-culture model to create *in vitro* prevascularized bone constructs. We hypothesized that a hypoxic stimulus will contribute to prevascularization of engineered bone. Bone marrow-derived MSCs and ECFCs from human adult peripheral blood were allowed to form co-culture pellets containing ECFCs and MSCs (1:4) or MSCs only in controls. After culture under normoxia or hypoxia (5%), pellets were harvested and processed for immunohistochemistry of CD31, α-smooth muscle actin, and osteocalcin. Expression of vascular endothelial growth factor and SDF-1α was analyzed by PCR to elucidate their involvement in hypoxic stimulation of prevascularization. The normoxic condition in co-cultures of MSCs and ECFCs supported the formation and maintenance of prevascular structures, including organized CD31-positive cells embraced by differentiated mural cells. These structures failed to form in hypoxic conditions, thereby rejecting the hypothesis that hypoxia stimulates prevasculogenesis in three-dimensional engineered bone constructs. Further, the formation of prevascular structures was paralleled by increased SDF-1α expression. It is suggested that actual oxygen levels were below 5% in the hypoxic co-cultures, which prevented prevascular structure formation. In conclusion, our normoxic co-culture model containing cells from clinically relevant sources sustained simultaneous endothelial, smooth muscle, and osteogenic differentiation.

Introduction

Engineered bone is considered a future option to fill osseous defects, as other bone replacements, such as autologous or allogeneic bone, are unavailable, insufficient, or associated with complications.[1–4] The size of engineered bone is currently confined by a maximum diffusion distance of nutrients and oxygen from the tissue surface or blood vessel toward the consuming cells.[5–8] *In vitro* prevascularized constructs have been previously created, a strategy already shown to accelerate functional anastomosis after *in vivo* implantation.[9] Organized functional networks have been obtained *in vivo* by combining an endothelial cell source, for example, cord blood and peripheral blood-derived endothelial progenitor cells (EPCs) or human umbilical vein endothelial cells (HUVECs), with a mural cell source, for example, multipotent stromal cells (MSCs) or smooth muscle cells, in matrigel plugs.[6,10–12] Previous studies focusing on prevascularized bone tissue engineering[13–17] have included several osteogenic cell sources, among which the primary osteoblasts[15,16] and the more proliferative MSCs[11,18] were most commonly used.

Several co-cultures contained EPCs, a term that has been collectively used in literature for several cell types, all expressing endothelial markers but with varying characteristics. Endothelial colony forming cells (ECFCs), formerly called "late EPC," are an attractive EPC population that can be obtained from human adult blood. This population is the only EPC type known to form functional vascular networks *de novo* in contrast to circulating angiogenic cells, formerly called "early EPCs," which are thought to stimulate angiogenesis in a paracrine manner.[14,19] Although endothelial cells and EPCs exhibited comparable angiogenic properties in monoculture,[20] EPCs (derived from the CD34+/CD133+ fraction from umbilical cord blood) were shown to be less hindered by the presence of osteoblasts than HUVECs in a sprouting assay.[21] In addition to this advantage, sufficient endothelial progenitors can be obtained from expanded isolates of adult peripheral blood, and they represent a clinically relevant cell source.[14]

The majority of co-culture studies has focused on the formation of prevascular structures rather than on osteogenic differentiation. Since the osteogenic tissue development is equally relevant, we assessed whether the formation of a

Departments of [1]Orthopaedics and [2]Nephrology and Hypertension, University Medical Center Utrecht, Utrecht, The Netherlands.
[3]Faculty of Veterinary Medicine, Utrecht University, Utrecht, The Netherlands.

prevascular structure would simultaneously allow osteogenic differentiation in human co-cultures.

Although hypoxia is considered a potent stimulator of angiogenesis, that is, blood vessel growth from pre-existing ones, through hypoxia inducible factor (HIF)-1α, considerably less consensus exists regarding the role of hypoxia in vasculogenesis. Vasculogenesis, *de novo* formation of a vascular network, is reported to be independent of oxygen tensions in embryogenesis;[22] however, postnatal vasculogenesis was shown to be driven by local ischemia.[23] Simultaneously, hypoxia is considered a strong inducer of progenitor cell recruitment and migration to create new vasculature.[23–25]

Therefore, we hypothesized that (i) hypoxia improves the development of prevascular networks in a three-dimensional osteogenic co-culture model, and that (ii) network formation is compatible with the osteogenic differentiation of the MSCs. The co-culture model consisted of adult human ECFCs and MSCs from peripheral blood and bone marrow of several donors, respectively.

Materials and Methods

MSC isolation and culture

Bone marrow aspirates were obtained from the iliac crests of patients undergoing a total hip replacement procedure after informed consent with approval of the local medical ethical committee (46 and 55 year old female donors and 48 and 72 year old male donors). The mononuclear cell fraction was isolated by centrifugation on Ficoll-paque and plated in a growth medium containing α-MEM (Gibco, 22561) supplemented with 0.2 mM L-ascorbic acid 2-phosphate (Sigma), 10% heat-inactivated fetal bovine serum (Biowhittaker), 100 units/mL penicillin with 100 μg/mL streptomycin (Gibco), and 1 ng/mL rhB-FGF (also: FGF-2; R&D Systems). Cells were passaged at subconfluence and seeded into the co-cultures at passages 3–5.

Multilineage potential of the passaged MSCs ($n=4$) was confirmed by differentiation into the adipogenic, osteogenic, and chondrogenic lineages as previously described.[26] Further, the MSCs were FACS-analyzed for the presence of established MSC markers and the absence of endothelial and hematopoietic markers.[27] Expression of CD73 (AD2, PE-conjugated; BD Pharmagen), CD90 (5 E10, Alexa647-conjugated; Biolegend), CD105 (MEM229, FITC-conjugated; Abcam), and W8B2 (PE-conjugated; Biolegend) was confirmed as well as the absence of CD31 (LCI-4, FITC-conjugated; Serotec), CD34 (581, FITC-conjugated; BD Pharmagen), and CD45 (HI30, PECy7-conjugated; BD Pharmagen). IgG-matched controls were purchased from Life Science. They were negative for CD31, CD34, and CD45, and showed >90% positivity for CD73, CD90, and CD105 (Supplementary Fig. S1; Supplementary Data are available online at www.liebertonline.com/tea).

ECFC isolation and culture

Adult peripheral blood (100 mL) was collected from volunteers and diluted 1:1 with PBS/2 mM EDTA. Mononuclear cells were isolated with Ficoll Paque PLUS (GE Healthcare) density gradient centrifugation and plated in endothelial growth medium (EGM) consisting of EGM-2 with 10% FCS and penicillin/streptomycin (Invitrogen) at a density of 50–150 * 10^6 cells/well in 12-well plates coated with 50 μg/mL rat tail collagen I (BD Biosciences). EGM was refreshed daily for 7 days and thrice a thereafter. Outgrowth of ECFC colonies was generally observed between 2 and 4 weeks. Colonies of ECFCs were trypsinized and replated in collagen-coated culture flasks and expanded in EGM until use. ECFC characterization was performed using flow cytometry by showing positivity for progenitor (CD34) and endothelial (VEGFR2, CD31, and CD144) markers, and absence of CD133, monocytic (CD14), and pan-leukocyte (CD45) markers (Supplementary Fig. S2A). In addition, ECFCs formed confluent cobblestone monolayers on collagen-coated plates and formed tube-like networks when plated on matrigel (Supplementary Fig. S2B, C). Generally, ECFCs of passage 3–6 were used for the co-culture experiments.

MSC/ECFC co-culture

The ratio of ECFCs over MSCs was determined to be optimal for our *in vitro* co-cultures when 20% ECFCs were included (Supplementary Fig. S3A). Comparable percentages of ECFCs (20%–40%) have also resulted in optimal *in vivo* vessel performance.[18] After expansion, cells were centrifuged to form co-culture pellets containing either ECFCs and MSCs (1:4) or MSCs only in controls. The pellets were maintained in osteogenic medium under either normoxic or hypoxic (2%–5% oxygen) conditions. The osteogenic differentiation medium (ODM) consisted of α-MEM supplemented with 10% heat-inactivated fetal bovine serum, 0.2 mM L-ascorbic acid 2-phosphate, 100 units/mL penicillin with 100 μg/mL streptomycin, 10 mM β-glycerophosphate, and 10 nM dexamethasone (Sigma; D8893). Further, the formation of prevascular structures and osteogenesis was studied in ODM, EGM, or in 1:1 mixtures of ODM and EGM (Supplementary Fig. S4). In addition, formation of prevascular structures was evaluated in pellets containing combinations of MSCs ($n=4$) and EPCs ($n=4$) from different donors. The pellets were harvested between 1 day and 4 weeks of culture.

Histology

Pellets were fixed in formalin and subsequently encapsulated in 4% alginate gel, dehydrated (graded ethanol), cleared in xylene, and embedded in paraffin for sectioning (5 μm). To detect mineralization, von Kossa staining was performed on the sections. In short, sections were deparaffinized and rehydrated before a 1-h incubation period in 5% silver nitrate (Fisher Scientific) under a light bulb. Unreacted silver was removed by submersion in 5% sodium thiosulphate (A17629; Alta Aesar). Cell nuclei were then counterstained with hematoxylin (Merck). The stained sections were examined by using a light microscope (Olympus BX51).

Immunohistochemistry

Immunohistochemical detection of the endothelial marker CD31, the mural cell marker α-smooth muscle actin (α-SMA), and osteogenic differentiation markers osteopontin and osteocalcin was performed on the sections. After deparaffinization and rehydration, sections were blocked in 0.3% H_2O_2 solution and also with 5% BSA in PBS for 30 min.

CD31-antigens were retrieved by boiling the sections in 10 mM citrate buffer (pH 6.0) for 15 min. These sections were incubated with the primary antibody for CD31 (1:20, monoclonal mouse, M0823; Dako) overnight at 4°C. Next, sections were incubated at room temperature with biotinylated secondary antibody (1:200, sheep anti-mouse, RPN1001v1; GE Healthcare). Finally, a simultaneous incubation of α-SMA (1:300, Cy3-conjugated, monoclonal mouse, C6198; Sigma) and Alexa Fluor 488-conjugated streptavidin (1:500, S32354; Invitrogen) was performed for 1 h at room temperature. Cell nuclei were stained with DAPI (1:100,000; Sigma).

For osteopontin and osteocalcin localization, antigen retrieval was performed by incubation with 1 mg/mL pronase (Sigma) and 10 mg/mL hyaluronidase (Sigma) for half an hour each. Next, sections were incubated with the primary antibodies for osteopontin (1:100, MPIIIB10_1, Developmental Studies Hybridoma Bank) and for osteocalcin (1:50, monoclonal mouse, OCG4; Alexis Biochemicals) at 4°C overnight. Then, the sections for osteopontin were incubated for an hour with the biotinylated goat anti-mouse antibody (1:200; GE Healthcare), before a 1-h incubation with horseradish peroxidase–conjugated streptavidin (1:500; Beckman Coulter). After the overnight primary antibody incubation, osteocalcin sections were incubated with GAM-HRP (1:200, goat anti-mouse, P0447; Dako) at room temperature for an hour. Both osteocalcin and osteopontin were detected by a 10-min conversion of 3,3′-diaminobenzidine solution (D5637; Sigma). Nuclei were counterstained with hematoxylin.

Isotype-matched controls were performed with mouse IgG1 monoclonal antibody (X0931; Dako) at concentrations comparable to those used for the stainings.

Image analysis

The freeware program AngioQuant (v1.33)[28] was used to calculate total lengths and number of junctions of the prevascular structures in CD31-stained sections. Before running the program, the images were modified in Adobe Photoshop CS3 Extended (version 10.0.1) to quench the blue hematoxylin staining that otherwise would interfere with structure detection by AngioQuant (all images are converted to grayscale). All images were processed with identical settings, including smoothening, segmentation with automatic thresholding, and pruning of structures below 10 pixels. The results were analyzed in Excel (Microsoft Office 2003) and normalized to the total area in each cross-section.

Blocking SDF-1α/CXCR4 signaling

To inhibit stromal-derived factor-1α or SDF-1α binding to CXCR4, the receptor antagonist AMD3100 (also known as Plerixafor, A5602; Sigma) was added to the medium before centrifuging the co-cultures into pellets. The co-cultures were maintained in ODM with AMD3100 thereafter and at every medium change, fresh AMD3100 was added. AMD3100 was used at concentrations of 0.1, 1, and 10 μg/mL, and control cultures received ODM without AMD3100. All cultures were harvested, fixed after 9 days, and processed for histology. Structure formation was analyzed on CD31-stained sections by AngioQuant. At least three sections of three cultures of identical conditions were included, and results were reproducible for another donor combination.

RT-PCR

Five identical pellets (quintuplicate) were pooled and homogenized in TriZol Reagent (Cat. No. 15596-018; Invitrogen Life Science Technologies), and RNA was extracted according to the manufacturer's protocol and quantified by spectrophotometry (ND-1000; Nanodrop technologies). To remove any genomic DNA contamination, isolated RNA was treated with TURBO DNase (Ambion) at 37°C for 30 min, followed by a denaturing step at 75°C for 10 min. Next, cDNA was synthesized from 500 ng total RNA (iScript cDNA synthesis kit; Bio-Rad) and diluted 10-fold in RNAse-free water.

Specific primers for platelet/endothelial cell adhesion molecule (*PECAM1* or *CD31*), vascular endothelial growth factor A (*VEGF-A*), chemokine (C-X-C motif) ligand 12 (*CXCL12* or *SDF-1α*), and *HIF-1α* were designed in primer3 online freeware (http://frodo.wi.mit.edu/primer3/) and are shown in Table 1, as well as primers for several housekeeping genes (*GAPDH, B2M, HPRT, PPIA, 18S,* and *P0*). Primers were designed to work at an annealing temperature of 60°C, in cases where primers functioned sub-optimally, the optimal annealing temperature was empirically established by setting a temperature gradient on the thermocycler.

The real-time PCR analysis was performed with iQ™ Sybr Green Supermix (Cat. No. 170-8885; Bio-Rad), conducted according to the instructions of the manufacturer. The final reaction volume was set at 15 μL. Triplicate samples were processed in MyIQ PCR system (Bio-Rad) and analyzed by using MyiQ System Software, Version 1.0.410 (Bio-Rad Laboratories Inc.). Data were analyzed by using the efficiency corrected Delta-Delta-Ct method.[29] The values of the genes of interest were normalized by using the geometric average of the values of the most stable housekeeping genes (*P0, HPRT,* and *PPIA*), selected by using the geNorm applet (http://medgen.ugent.be/~jvdesomp/genorm/).[30] Expression values were subsequently calculated across biological replicates by using an experiment-mean centered approach,[31] corresponding p-values were calculated by using one-way analysis of variance (ANOVA) and Tukey's *post-hoc* test.

Statistical analyses

Significant differences of the means were detected by ANOVA with subsequent posthoc Tukey HSD analysis, where $p < 0.05$ was considered significant. The significance of the difference of the means ($n = 5$–8) between normoxic and hypoxic groups of the AngioQuant data was determined by Student's *t*-tests. All calculations were carried out in SPSS 15.0. All graphs represent means with their standard deviations.

Results

Prevascular structures do not develop under hypoxic conditions

Control cultures, solely consisting of MSCs, did not develop any CD31-positive cell or structure within 22 days (Fig. 1D, inset). In co-culture pellets maintained under ambient oxygen tension (normoxia), organization of endothelial cells into prevascular structures did occur at 12 and 22 days of culture (Fig. 1A, C). However, when the co-cultures were

Table 1. Primer Sequences Used for Quantitative Real-Time Polymerase Chain Reaction

Gene symbol	*Accession ID*	*Forward primers (5′ to 3′)*	T_m, *calculated* (°C)	*Reverse primers (5′ to 3′)*	T_m, *calculated* (°C)	$T_{annealing}$ (°C)
PECAM1	NM_000442	GCAGTGGTTATCATCGGAGTG	59	TCGTTGTTGGAGTTCAGAAGTG	59	60
VEGFA	NM_001025366	CCACCACACCATCACCATC	59	GCGAATCCAATTCCAAGAGG	60	56
CXCL12	NM_199168	TTGTGAGAGATGAAAGGG	50	TACCGTATGCTATAAATGC	49	56
HIF1A	NM_001530	AGCCGAGGAAGAACTATGAAC	56	ATTTGATGGGTGAGGAATGGG	62	63
GAPDH	NM_002046	ACAGTCAGCCGCATCTTC	56	GCCCAATACGACCAAATCC	59	56
HPRT1	NM_000194	TGACACTGGCAAAACAATGCA	62	GGTCCTTTTCACCAGCAAGCT	61	60
RN18S1	NR_003286	GGCGCCCCCTCGATGCTCTTAG	71	GCTCGGGCCTGCTTTGAACACTCT	69	56
RPLP0	NM_001002	TGCACAATGGCAGCATCTAC	59	ATCCGTCTCCACAGACAAGG	59	60
B2M	NM_004048	TACTCCAAAGATTCAGGTTTACTC	55	TTCACACGGCAGGCATAC	58	60
PPIA	NM_021130	ATGGTCAACCCCACCGTGT	62	TCTGCTGTCTTTGGGACCTTGTC	64	60

kept under hypoxia, the CD31-positive cells remained diffusely scattered as single cells throughout the pellets at 12 and 22 days of culture (Fig. 1B, D).

These results were reproducible for pellets consisting of MSCs and ECFCs derived from different donors (including co-cultures containing cord blood-derived ECFCs, of which representative images are shown in Supplementary Fig. S3B). Strikingly, of all donor-combinations that had been assessed (4 MSC donors and 3 ECFC from peripheral blood and 1 from cord blood), a few did not show formation of a prevascular structure. The latter co-cultures contained MSCs from one particular donor.

The effect of hypoxia was also reflected in the quantitative assessment of the formation of structures. The total length of all structures and the total number of structure junctions per μm^2 were significantly elevated (2.4-fold and 6.2-fold, respectively) in the normoxic sections (Fig. 1K, L).

Double staining of CD31 and α-SMA, indicative for mural cells, revealed that α-SMA-positive cells were lining the CD31-positive prevascular structures in the co-cultures (Fig. 1E–I). Additionally, the α-SMA expressing cells contained the elongated nuclear shapes characteristic for smooth muscle cells (Fig. 1J, K, arrowheads).

Osteogenic markers are expressed in normoxic and hypoxic conditions

The osteogenic marker osteopontin is expressed in both normoxic and hypoxic co-cultures by day 22 (Fig. 2A, B). Overall, more cells produced osteopontin in the normoxic compared with hypoxic cultures at an early time point. Similarly, osteocalcin was expressed in co-cultures from both conditions at day 22 (not shown). In contrast, matrix mineralization of co-cultures appeared earlier under hypoxia when compared with normoxia. By day 22, both normoxic and hypoxic co-cultures had deposited mineralized spots and formed mineralized nodules (Fig. 2C, D).

Formation of prevascular structures and osteogenesis exclusively co-occur in osteogenic conditions

The medium composition was varied to determine which minimal requirements in growth factors would optimally support both the formation of prevascular structures and osteogenic differentiation under normoxic conditions. Co-culture pellets were maintained in EGM, ODM or in a 1:1 mixture of both. Control pellets were cultured in ODM only. Staining of CD31-positive cells at day 7 revealed that prevascular structures were able to assemble in all three media tested (Fig. 3A–D), whereas the control culture was negative for CD31 (MSCs only). In addition, mineralization of the cultures was assessed at day 28 to show their osteogenic potential (Fig. 3E–H). Only when cultured in ODM, the control and co-culture had deposited calcium phosphates into the extracellular matrix. Therefore, ODM was the only medium that supported both vasculogenesis and osteogenesis under normoxia.

Involvement of SDF-1 signaling in in vitro *vasculogenesis*

The expression levels of several genes were evaluated on day 7 in both control cultures (MSC only) and co-cultures. In

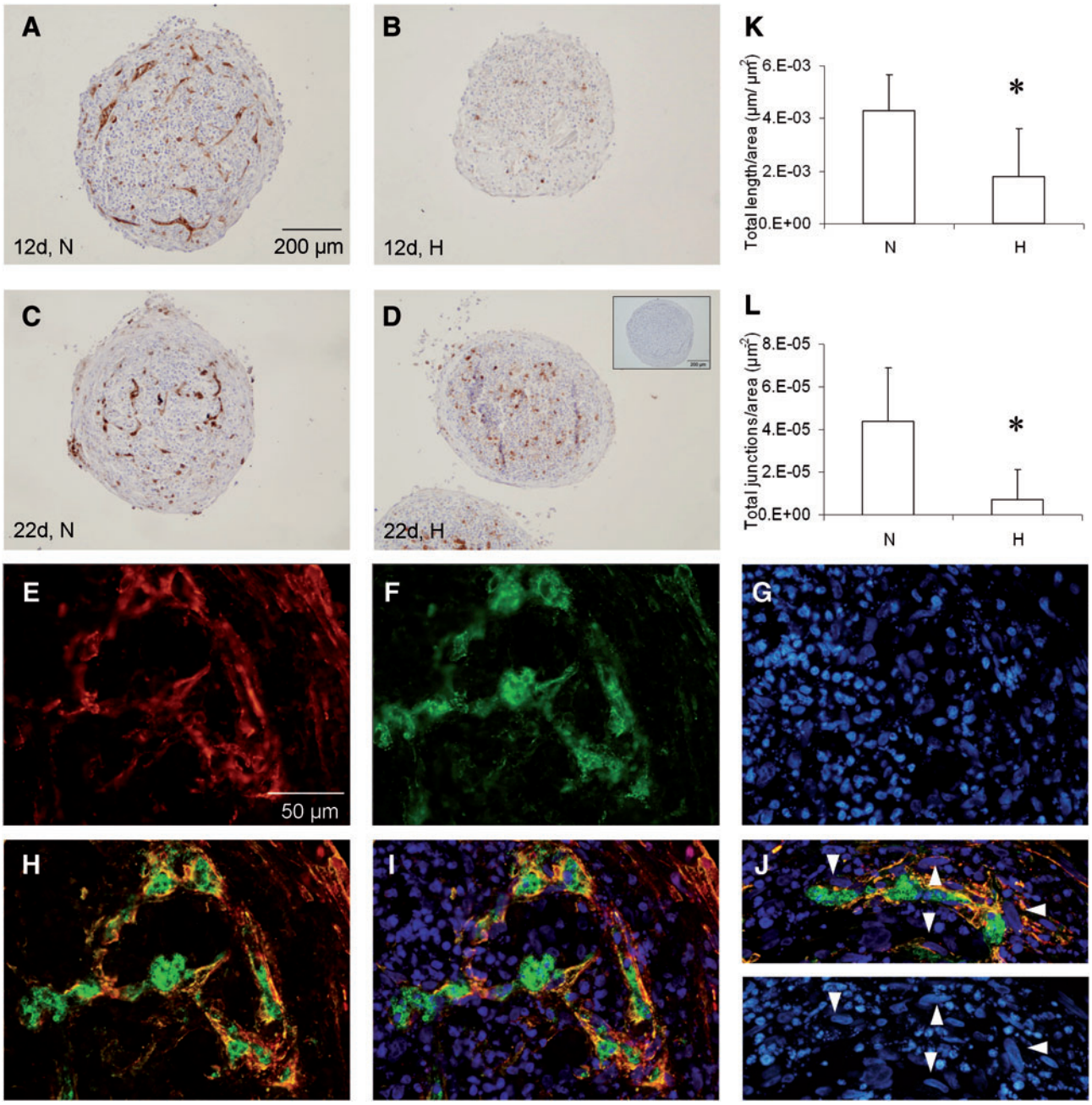

FIG. 1. The influence of oxygen tensions on the formation of prevascular structures in MSC/ECFC co-cultures. CD31 immunostaining of pellets at 12 days **(A, B)** and 22 days **(C, D)** consisting of MSC and ECFCs. The pellets were cultured at either normoxia **(**N in **A, C)** or hypoxia **(**H in **B, D)**. Only pellets containing ECFCs and cultured under normoxia demonstrate formation of tubular structures. Sections were counterstained with hematoxylin. Control pellets containing MSCs only were negative **(**inset in **D)**. The total length **(K)** and total number of junctions **(L)** of the CD31-positive structures normalized to total section area were significantly increased for the normoxic co-cultures ($^*p < 0.05$). Localization of α-smooth muscle actin **(E)** around CD31-positive structures **(F)**, with an overlay in **(H)** and **(I)** and nuclear counterstain in **(G)**. **(J)** Elongated nuclei (arrowheads) typical for smooth muscle cell differentiation were observed in the α-smooth muscle actin (red) cells. Scale bar in **(A)** denotes scale for **A–D**, whereas bar in **(E)** represents the scale for **E–J**. ECFC, endothelial colony forming cell; MSC, multipotent stromal cell. Color images available online at www.liebertonline.com/tea

contrast to our hypothesis that hypoxia stimulates prevascularization, expression of *HIF-1α, CD31,* and *SDF-1α* was increased when the co-cultures were exposed to normoxic conditions rather than to hypoxic conditions at day 7 (Fig. 4A). However, *VEGF* gene expression was elevated in control cultures under hypoxia at day 7, whereas in co-cultures, *VEGF* expression levels were not affected by hypoxia. In contrast, the levels of VEGF protein were reduced in the hypoxic co-cultures compared with normoxic co-cultures and control cultures, as determined by an ELISA in the culture medium at both day 3 and 7 (Quantikine kit DVE00 from R&D Systems, Fig. 4B, $n = 1$). SDF-1α protein release

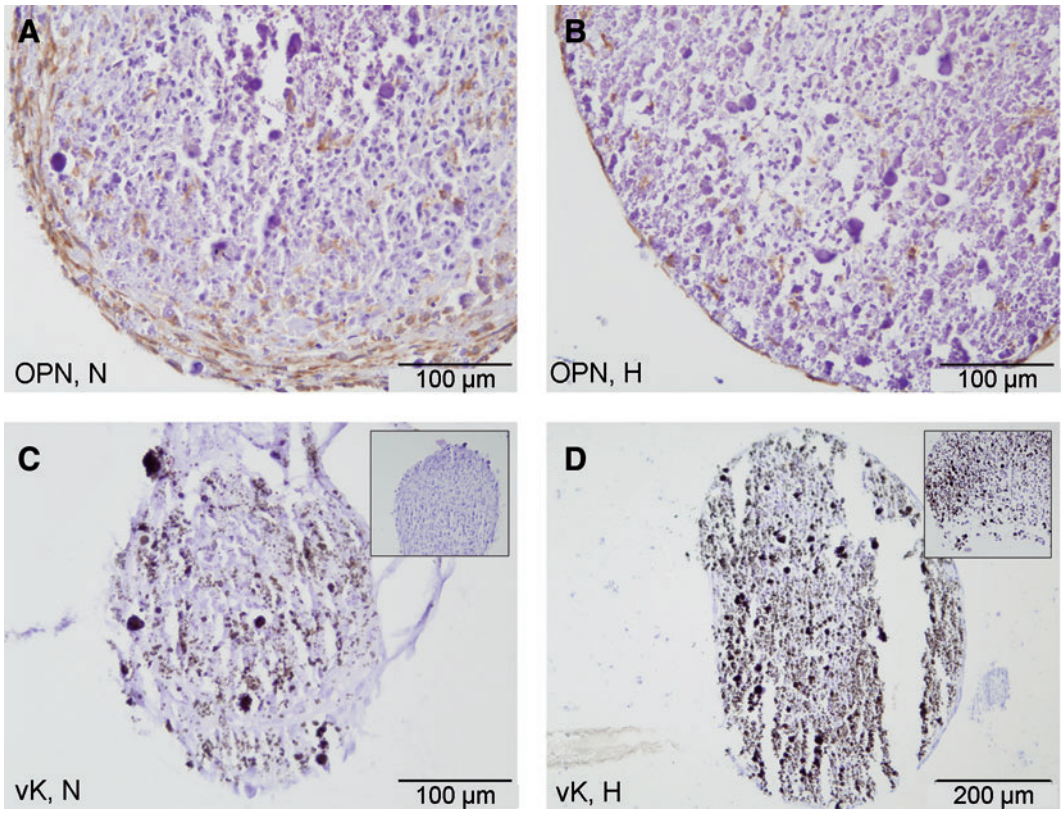

FIG. 2. Osteogenic differentiation of co-cultures under normoxic **(**N in **A, C)** and hypoxic conditions **(**H in **B, D)**. Expression of osteopontin (OPN) at day 22 of culture **(A, B)**. Von Kossa (vK) staining indicates mineral depositions in black at day 22 of culture **(C, D)**. Insets show extent of mineralization at day 12. Color images available online at www.liebertonline.com/tea

into the culture medium was not detectable with a Quantikine ELISA kit (DSA00; R&D Systems).

Elevated RNA expression levels of *HIF-1α* and its downstream target *SDF-1α* corresponded with increased *CD31* expression in the normoxic co-cultures (Fig. 4). Since these were the cultures in which the structures had formed, the involvement of SDF-1α signaling in *in vitro* vasculogenesis was assessed. To this end, SDF-1α binding to its specific receptors CXCR4 and CXCR7[32,33] was blocked by addition of AMD3100 in different concentrations (0–10 μg/mL).[34–37] Although the total length and size of the prevascular structures was not significantly altered when AMD3100 was present in

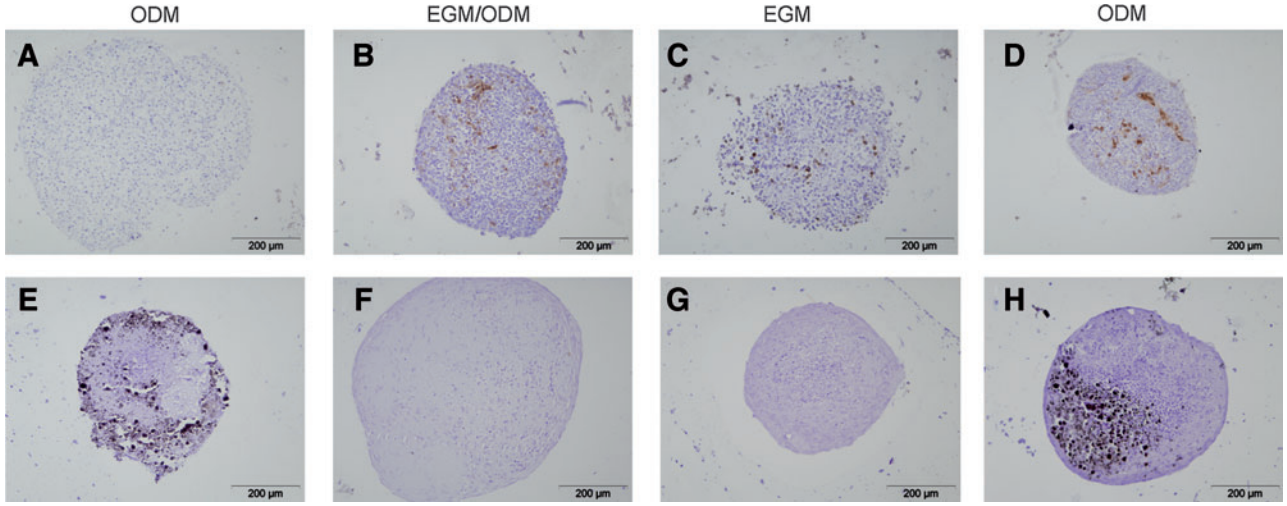

FIG. 3. Medium-based variation in the formation of prevascular structures **(A–D**, CD31, 7 days**)** and mineralization **(E–H**, von Kossa, 28 days**)** of co-cultures in three different media. Control pellets, containing MSCs only, were cultured in osteogenic differentiation medium **(A, E)**. MSC/endothelial progenitor cell co-culture pellets were maintained in either 1:1 osteogenic/endothelial medium **(B, F)**; endothelial medium **(C, G)**; or osteogenic medium **(D, H)**. Images are representative for pellets from three donor combinations, all cultured in normoxic conditions. Color images available online at www.liebertonline.com/tea

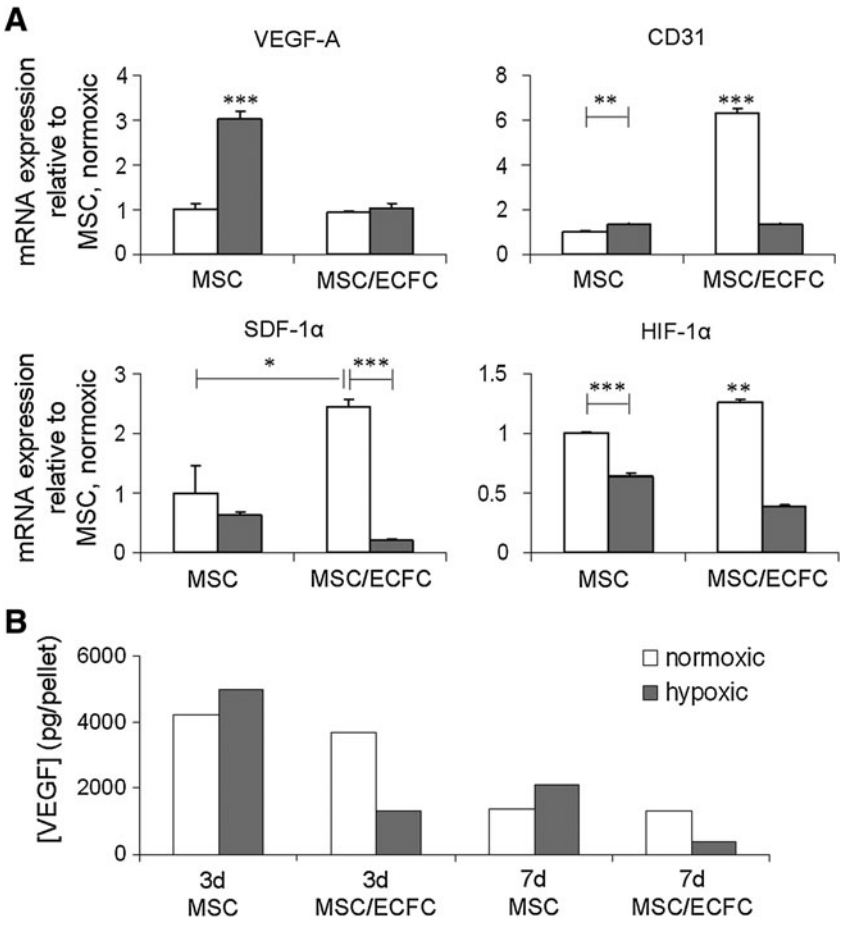

FIG. 4. The influence of co-culture and oxygen tensions on gene and protein expression levels. **(A)** Gene expression of controls and co-cultures, normalized to *P0, HPRT,* and *PPIA* expression levels are expressed as fold-increase relative to the MSC only expression in normoxic (N) conditions ($n=3$). Normoxic groups are shown in white, and hypoxic groups are shown in gray. The co-cultures were maintained in osteogenic medium for 7 days (*$p<0.05$; **$p<0.01$; ***$p<0.001$; asterisks located above a column indicate a significant difference compared with all other groups). **(B)** VEGF protein release into the culture medium after 3 and 7 days for MSCs or co-cultures (MSC/ECFC, $n=1$). VEGF, vascular endothelial growth factor.

the medium (Fig. 5I, J), local aggregation of CD31-positive cells was present in several sections from the co-cultures that were treated with AMD3100 (Fig. 5F inset, H).

Discussion

In the current study, we investigated the involvement of a hypoxic stimulus in vasculogenesis of a tissue-engineered bone model. In contrast to our hypothesis, the level of hypoxia introduced here did not allow the formation of a prevascular structure, whereas normoxic culture conditions did. We postulate here that our normoxic condition most likely represented a hypoxic environment for the cells. Oxygen tensions actually sensed by the cells inside the pellets are dependent on a declining gradient toward the tissue center,[8] which is caused by cellular oxygen consumption. The hypoxic conditions in the normoxic cultures may, therefore, have caused upregulation of hypoxic markers. Oxygen tensions experienced by the cells in the center of hypoxic cultures may have been well below the imposed hypoxic oxygen tensions of 2%–5%, as the maximum diffusion distance of nutrients and oxygen in tissues was estimated to be 200 μm from the capillaries in tissues.[38,39] The size of the pellets (ranging from 0.7 to 1.5 mm) exceeded these dimensions. In turn, these low oxygen tensions may have initiated oxygen conformance[40–42] and as such suppressed cellular processes, including those associated with vasculogenesis. The absence of vascular structures in hypoxic co-cultures confirms the findings obtained in a co-culture model of endothelial cells (HUVEC) and fibroblasts, where hypoxia severely limited capillary formation by a mechanism independent from VEGF signaling.[43] The stimulation of structure formation was attributed to the production of an unknown factor (other than VEGF or FGF-2) that is produced under normoxic conditions and sensitive to hypoxia.

Vasculogenesis is the process that is responsible for *de novo* blood vessel formation, both during embryogenesis and after birth.[44,45] The formation of the initial vascular plexus during embryology is thought to take place independently from hypoxic gradients.[22] In contrast, the subsequent organization of capillaries is orchestrated by local tissue oxygen tensions. The hypoxic conditions are considered to be a strong recruitment and migration stimulus for EPCs or ECFCs.[23–25] During hypoxic conditions, HIF-1α is stabilized, which leads to increased SDF-1α (stromal derived factor 1α) expression. SDF-1α was implicated as the mediator of hypoxia in terms of endothelial cell recruitment.[23–25] The mediatory pathway was shown to act independently from the VEGF, thus signaling cascade. The latter is another downstream target of HIF-1α. Nevertheless, SDF-1α was reported to be a stronger stimulus for vasculogenesis than VEGF in a murine model.[46] Therefore, the effects of hypoxia on the formation of prevascular structures was studied by monitoring changes in *HIF-1α, VEGF,* and *SDF-1α* levels.

The expression of *SDF-1α* was increased in the normoxic co-cultures that formed prevascular structures, thus

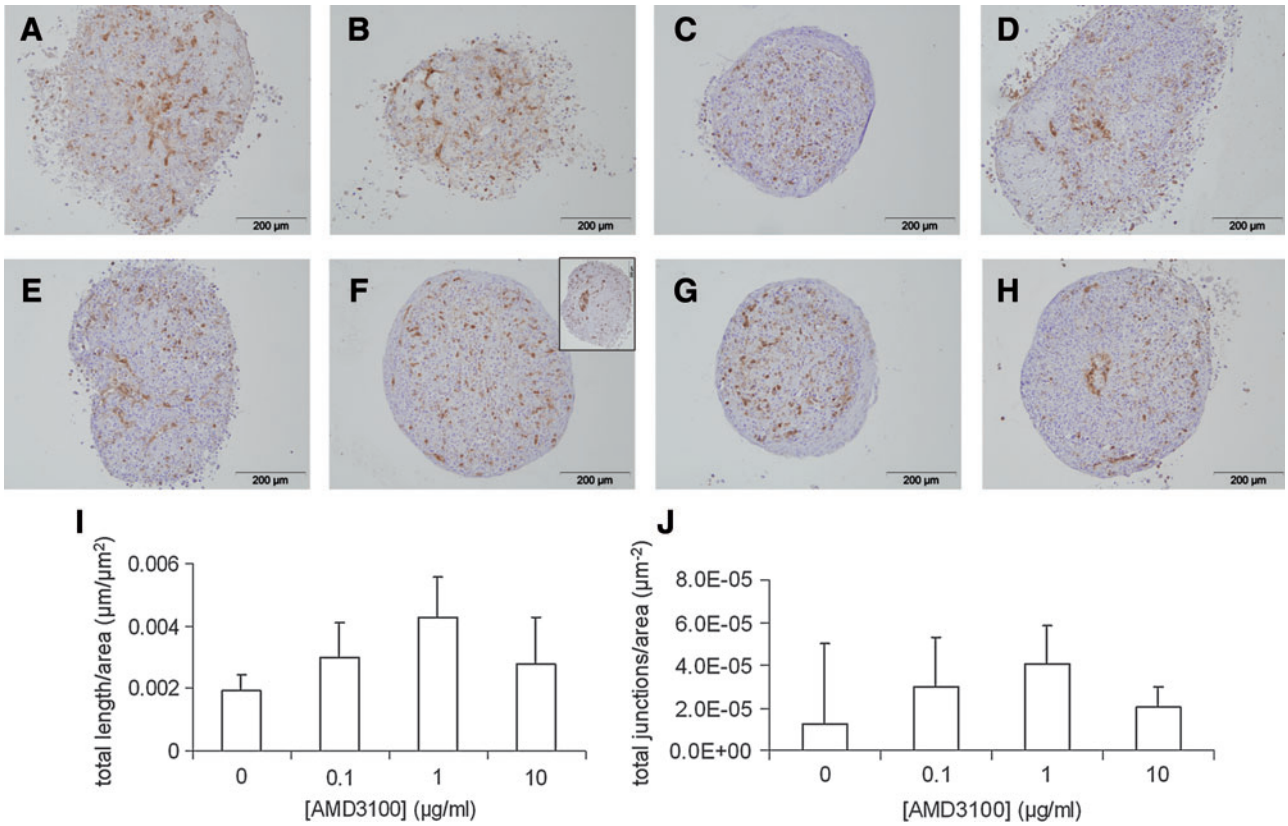

FIG. 5. Effects of AMD3100 on formation of prevascular structures in co-cultures at 9 days in normoxic conditions. **(A)** CD31 is detected in brown in co-culture sections from duplicate pellets that were maintained in 0 **(A, E)**; 0.1 **(B, F)**; 1 **(C, G)**; 10 **(D, H)** µg AMD3100 per mL osteogenic medium. The inset in **(F)** is showing another section with a local aggregation of CD31-positive cells, as also demonstrated in **(H)**. **(I, J)** Total length and number of junctions of the CD31-positive structures were quantified in AngioQuant and normalized to the section area. No significant differences among the groups were detected ($n=3$). Color images available online at www.liebertonline.com/tea

suggesting an association of this factor with the prevascular assembly. The involvement of SDF-1α in the vasculogenic process was studied by addition of AMD3100 to the co-cultures to block the SDF-1α receptors CXCR4 and CXCR7, the latter of which was only recently identified as a receptor for SDF-1α.[47] The expression of both receptors was shown on MSCs and increased under hypoxia (3% oxygen).[48] Although the presence of CXCR4 on vascular and hematopoietic progenitors was described, the expression of CXCR7 by ECFCs is still unknown.[24,46,49] However, the extent of formation of prevascular structures was not significantly affected by the presence of AMD3100.

The fact that the formation of prevascular structures was not affected by AMD3100 may either be caused by the fact that SDF-1α is not, or only partly, involved in this process or that the effect of the inhibitor was masked by one of the following reasons. First, it is possible that SDF-1α is not involved in the *in vitro* vasculogenic process in the co-culture model. Second, AMD3100 toxicity may have affected vasculogenesis. Although toxic effects have been reported for high concentrations of AMD3100, the concentrations used in the current study were shown to support cell survival for >90% for G3H cells.[37] Another mechanism may be associated with the actions of AMD3100 on CXCR4 and CXCR7. It is known that AMD3100 is a receptor antagonist of CXCR4 and that it does not induce its signaling. However, the other SDF-1α receptor, CXCR7, was recently reported to be allosterically activated by AMD3100.[34] Therefore, the apparent absence of blocking of vasculogenesis that was observed in our co-cultures, even at high concentrations of AMD3100, might be masked by enhanced CXCR7-linked signaling pathways.[34]

The transcription of the other hypoxia-inducible gene, *VEGF*, was low and not affected by hypoxia in the co-cultures. As mentioned earlier, prevascular structures were reported to assemble preferably under normoxic conditions, but this effect was thought to be controlled by a VEGF-independent pathway.[43] This may explain the unrelated expression of *VEGF* in the current study. In our co-cultures, not only the *VEGF* mRNA levels but also the expression of VEGF protein were low by day 7. In our data, even a tendency toward decreased VEGF protein expression in hypoxic compared with normoxic co-cultures was observed. Since mRNA levels are not directly correlated to protein expression, the changes in mRNA levels of *VEGF* precede protein production, and the two may slightly differ at the same time point.

A novel finding presented here was the dependence of the formation of a prevascular structure on MSC characteristics. Out of several combinations of both MSCs and EPCs isolated from four different donors each, only combinations containing MSCs from one particular donor did not show

prevascular organization. So far, this phenomenon has not been described. If this is reproducible in an *in vivo* model, then the *in vitro* model may present a predictive tool that can be used before application in clinical practice or animal experiments.

Hypoxic conditions are known to predominantly inhibit the osteogenic differentiation of MSCs,[50–52] whereas enhancement of osteogenesis is rarely reported.[53] Species and oxygen tensions varied among these experiments, which may have caused their different outcomes. In the current study, MSCs were combined with ECFCs, and it was expected that hypoxia (5% oxygen) would not hinder osteogenesis of the MSCs. From our qualitative observations of osteogenesis, it can be concluded that expression of osteogenic proteins osteopontin and osteocalcin proceeded similarly in co-cultures exposed to normoxic and hypoxic conditions. However, mineralization was present in hypoxic co-cultures before it occurred in normoxic cultures. The early onset of mineralization and, thus, osteogenesis in our study disagrees with the majority of previous studies. However, in our model, ECFCs were in co-culture with the MSCs. Expression levels of *HIF-1α* were elevated in our hypoxic co-cultures, accompanied by increased VEGF protein release. It is known that VEGF stimulates endothelial cells to form prevascular structures. They, in turn, can stimulate osteogenesis.[54,55]

The ability of the cells in the *in vitro* co-culture model to simultaneously form endothelial networks with mural cell lining and osteogenic differentiation has not been demonstrated so far. Several studies have shown that mural cell differentiation can occur in a co-culture of endothelial (progenitor) cells and bone (progenitor) cells in *in vivo* models.[6,10,11,56] In addition, recently, the feasibility of the co-culture model from clinically relevant sources, such as the bone marrow-derived MSCs and HUVECs, to anastomose to a host's vasculature was demonstrated.[56] The MSCs were separately differentiated toward the osteogenic lineage or into pericytes and combined with HUVECs in a collagen/fibronectin gel. However, our *in vitro* model shows more efficient differentiation into three lineages in only osteogenic medium. Moreover, the clinical application of peripheral blood-derived endothelial progenitors is favorable compared with the use of HUVECs. ECFCs cannot only be derived from an autologous source; they also demonstrate more favorable proliferative potential and improved formation of vascular structures.

Altogether, combination of MSCs and ECFCs from clinically relevant human adult sources, such as the bone marrow and peripheral blood, is a promising means to realize the creation of large engineered bone constructs.

Conclusion

We demonstrated for the first time that a prevascular structure including endothelial arrangement and differentiated mural cells can be created among osteogenically differentiating cells. In addition, the differentiation into these three distinct cell types was achieved under normoxic, osteogenic conditions from clinically highly relevant cell sources. The next steps toward clinical application demands conquering the hurdle of increasing the size of prevascularized constructs and controlling donor-dependent outcomes.

Acknowledgments

This work is a part of the UMC Utrecht strategic program on Regenerative Medicine. The authors gratefully acknowledge the support of the Smart Mix Program of the Netherlands Ministry of Economic Affairs and the Netherlands Ministry of Education, Culture, and Science. M.C. Verhaar is supported by a grant from the Netherlands Organization for Scientific Research (NWO Vidi grant number 016.096.359). The antibody against osteopontin, developed by M. Solursh and A. Franzen, was obtained from the DSHB developed under the auspices of the NICHD and maintained by The University of Iowa, Department of Biology, Iowa City, IA 52242. The authors are grateful to Willy Noort for providing the antibodies and her assistance in the FACS characterization of MSCs, and to Hendrik Gremmels for his excellent assistance in RT-PCR data analysis.

Disclosure Statement

No competing financial interests exist.

References

1. Kneser, U., *et al.* Tissue engineering of bone: the reconstructive surgeon's point of view. J Cell Mol Med **10,** 7, 2006.
2. Arrington, E.D., *et al.* Complications of iliac crest bone graft harvesting. Clin Orthop Relat Res **(329),** 300, 1996.
3. Banwart, J.C., Asher, M.A., and Hassanein, R.S. Iliac crest bone graft harvest donor site morbidity. A statistical evaluation. Spine (Phila Pa 1976) **20,** 1055, 1995.
4. Ebraheim, N.A., Elgafy, H., and Xu, R. Bone-graft harvesting from iliac and fibular donor sites: techniques and complications. J Am Acad Orthop Surg **9,** 210, 2001.
5. Griffith, L.G., and Naughton, G. Tissue engineering—current challenges and expanding opportunities. Science **295,** 1009, 2002.
6. Melero-Martin, J.M., *et al.* In vivo vasculogenic potential of human blood-derived endothelial progenitor cells. Blood **109,** 4761, 2007.
7. Rouwkema, J., Rivron, N.C., and van Blitterswijk, C.A. Vascularization in tissue engineering. Trends Biotechnol **26,** 434, 2008.
8. Volkmer, E., *et al.* Hypoxia in static and dynamic 3D culture systems for tissue engineering of bone. Tissue Eng Part A **14,** 1331, 2008.
9. Chen, X., *et al.*, Prevascularization of a fibrin-based tissue construct accelerates the formation of functional anastomosis with host vasculature. Tissue Eng Part A **15,** 1363, 2009.
10. Koike, N., *et al.* Tissue engineering: creation of long-lasting blood vessels. Nature **428,** 138, 2004.
11. Sanz, L., *et al.* Long-term in vivo imaging of human angiogenesis: critical role of bone marrow-derived mesenchymal stem cells for the generation of durable blood vessels. Microvasc Res **75,** 308, 2008.
12. Hirschi, K.K., Rohovsky, S.A., and D'Amore, P.A. PDGF, TGF-beta, and heterotypic cell-cell interactions mediate endothelial cell-induced recruitment of 10T1/2 cells and their differentiation to a smooth muscle fate. J Cell Biol **141,** 805, 1998.
13. Rouwkema, J., de Boer, J., and Van Blitterswijk, C.A. Endothelial cells assemble into a 3-dimensional prevascular network in a bone tissue engineering construct. Tissue Eng **12,** 2685, 2006.
14. Rouwkema, J., *et al.* The use of endothelial progenitor cells for prevascularized bone tissue engineering. Tissue Eng Part A **15,** 2015, 2009.

15. Fuchs, S., *et al.* Contribution of outgrowth endothelial cells from human peripheral blood on in vivo vascularization of bone tissue engineered constructs based on starch polycaprolactone scaffolds. Biomaterials **30,** 526, 2009.
16. Fuchs, S., *et al.* Dynamic processes involved in the pre-vascularization of silk fibroin constructs for bone regeneration using outgrowth endothelial cells. Biomaterials **30,** 1329, 2009.
17. Usami, K., *et al.* Composite implantation of mesenchymal stem cells with endothelial progenitor cells enhances tissue-engineered bone formation. J Biomed Mater Res A **90,** 730, 2009.
18. Melero-Martin, J.M., *et al.* Engineering robust and functional vascular networks in vivo with human adult and cord blood-derived progenitor cells. Circ Res **103,** 194, 2008.
19. Sieveking, D.P., *et al.* Strikingly different angiogenic properties of endothelial progenitor cell subpopulations: insights from a novel human angiogenesis assay. J Am Coll Cardiol **51,** 60, 2008.
20. Finkenzeller, G., *et al.* In vitro angiogenesis properties of endothelial progenitor cells: a promising tool for vascularization of ex vivo engineered tissues. Tissue Eng **13,** 1413, 2007.
21. Stahl, A., *et al.* Endothelial progenitor cell sprouting in spheroid cultures is resistant to inhibition by osteoblasts: a model for bone replacement grafts. FEBS Lett **579,** 5338, 2005.
22. Semenza, G.L. Vasculogenesis, angiogenesis, and arteriogenesis: mechanisms of blood vessel formation and remodeling. J Cell Biochem **102,** 840, 2007.
23. Li, B., *et al.* VEGF and PlGF promote adult vasculogenesis by enhancing EPC recruitment and vessel formation at the site of tumor neovascularization. Faseb J **20,** 1495, 2006.
24. Ceradini, D.J., and Gurtner, G.C. Homing to hypoxia: HIF-1 as a mediator of progenitor cell recruitment to injured tissue. Trends Cardiovasc Med **15,** 57, 2005.
25. Ceradini, D.J., *et al.* Progenitor cell trafficking is regulated by hypoxic gradients through HIF-1 induction of SDF-1. Nat Med **10,** 858, 2004.
26. Pittenger, M.F., *et al.* Multilineage potential of adult human mesenchymal stem cells. Science **284,** 143, 1999.
27. Dominici, M., *et al.* Minimal criteria for defining multipotent mesenchymal stromal cells. The International Society for Cellular Therapy position statement. Cytotherapy **8,** 315, 2006.
28. Niemisto, A., *et al.* Robust quantification of in vitro angiogenesis through image analysis. IEEE Trans Med Imaging **24,** 549, 2005.
29. Pfaffl, M.W. A new mathematical model for relative quantification in real-time RT-PCR. Nucleic Acids Res **29,** e45, 2001.
30. Vandesompele, J., *et al.* Accurate normalization of real-time quantitative RT-PCR data by geometric averaging of multiple internal control genes. Genome Biol **3,** RESEARCH0034, 2002.
31. Kubota, Y., *et al.* Role of laminin and basement membrane in the morphological differentiation of human endothelial cells into capillary-like structures. J Cell Biol **107,** 1589, 1988.
32. Valentin, G., Haas, P., and Gilmour, D. The chemokine SDF1a coordinates tissue migration through the spatially restricted activation of Cxcr7 and Cxcr4b. Curr Biol **17,** 1026, 2007.
33. Thelen, M., and Thelen, S. CXCR7, CXCR4 and CXCL12: an eccentric trio? J Neuroimmunol **198,** 9, 2008.
34. Kalatskaya, I., *et al.* AMD3100 is a CXCR7 ligand with allosteric agonist properties. Mol Pharmacol **75,** 1240, 2009.
35. Kawaguchi, A., *et al.* Inhibition of the SDF-1alpha-CXCR4 axis by the CXCR4 antagonist AMD3100 suppresses the migration of cultured cells from ATL patients and murine lymphoblastoid cells from HTLV-I Tax transgenic mice. Blood **114,** 2961, 2009.
36. Yin, Y., *et al.* AMD3100 mobilizes endothelial progenitor cells in mice, but inhibits its biological functions by blocking an autocrine/paracrine regulatory loop of stromal cell derived factor-1 in vitro. J Cardiovasc Pharmacol **50,** 61, 2007.
37. Yoshida, D., *et al.* The CXCR4 antagonist AMD3100 suppresses hypoxia-mediated growth hormone production in GH3 rat pituitary adenoma cells. J Neurooncol **100,** 51, 2010.
38. Carrier, R.L., *et al.* Perfusion improves tissue architecture of engineered cardiac muscle. Tissue Eng **8,** 175, 2002.
39. Muschler, G.F., Nakamoto, C., and Griffith, L.G. Engineering principles of clinical cell-based tissue engineering. J Bone Joint Surg Am **86-A,** 1541, 2004.
40. Subramanian, R.M., *et al.* Hypoxic conformance of metabolism in primary rat hepatocytes: a model of hepatic hibernation. Hepatology **45,** 455, 2007.
41. Simon, M.C., *et al.* Hypoxia-induced signaling in the cardiovascular system. Annu Rev Physiol **70,** 51, 2008.
42. Arthur, P.G., Giles, J.J., and Wakeford, C.M. Protein synthesis during oxygen conformance and severe hypoxia in the mouse muscle cell line C2C12. Biochim Biophys Acta **1475,** 83, 2000.
43. Griffith, C.K., and George, S.C. The effect of hypoxia on in vitro prevascularization of a thick soft tissue. Tissue Eng Part A **15,** 2423, 2009.
44. Rafii, S., and Lyden, D. Therapeutic stem and progenitor cell transplantation for organ vascularization and regeneration. Nat Med **9,** 702, 2003.
45. Kassmeyer, S., *et al.* New insights in vascular development: vasculogenesis and endothelial progenitor cells. Anat Histol Embryol **38,** 1, 2009.
46. Aghi, M., *et al.* Tumor stromal-derived factor-1 recruits vascular progenitors to mitotic neovasculature, where microenvironment influences their differentiated phenotypes. Cancer Res **66,** 9054, 2006.
47. Burns, J.M., *et al.* A novel chemokine receptor for SDF-1 and I-TAC involved in cell survival, cell adhesion, and tumor development. J Exp Med **203,** 2201, 2006.
48. Liu, H., *et al.* Hypoxic preconditioning advances CXCR4 and CXCR7 expression by activating HIF-1alpha in MSCs. Biochem Biophys Res Commun 401, 509, 2010.
49. Maksym, R.B., *et al.* The role of stromal-derived factor-1—CXCR7 axis in development and cancer. Eur J Pharmacol **625,** 31, 2009.
50. D'Ippolito, G., *et al.* Low oxygen tension inhibits osteogenic differentiation and enhances stemness of human MIAMI cells. Bone **39,** 513, 2006.
51. Fehrer, C., *et al.* Reduced oxygen tension attenuates differentiation capacity of human mesenchymal stem cells and prolongs their lifespan. Aging Cell **6,** 745, 2007.
52. Potier, E., *et al.* Hypoxia affects mesenchymal stromal cell osteogenic differentiation and angiogenic factor expression. Bone **40,** 1078, 2007.

53. Lennon, D.P., Edmison, J.M., and Caplan, A.I. Cultivation of rat marrow-derived mesenchymal stem cells in reduced oxygen tension: effects on in vitro and in vivo osteochondrogenesis. J Cell Physiol **187,** 345, 2001.
54. Grellier, M., Bordenave, L., and Amedee, J. Cell-to-cell communication between osteogenic and endothelial lineages: implications for tissue engineering. Trends Biotechnol **27,** 562, 2009.
55. Stahl, A., *et al.* Bi-directional cell contact-dependent regulation of gene expression between endothelial cells and osteoblasts in a three-dimensional spheroidal coculture model. Biochem Biophys Res Commun **322,** 684, 2004.
56. Tsigkou, O., *et al.* Engineered vascularized bone grafts. Proc Natl Acad Sci USA **107,** 3311, 2010.

Address correspondence to:
Gawlitta Debby, Ph.D.
Department of Orthopaedics
University Medical Center Utrecht
PO Box 85500
3508 GA Utrecht
The Netherlands

E-mail: d.gawlitta@umcutrecht.nl

Received: December 16, 2010
Accepted: August 19, 2011
Online Publication Date: September 28, 2011